

Physico-chemical and Biosafety Evaluations of a Polyurethane Carrier Used for Bevacizumab

RAMONA CARMEN ALBULESCU¹, LIVIA-CRISTINA BORCAN^{2*}, FLORIN BORCAN³

¹ “Victor Babes” University of Medicine and Pharmacy, Faculty of Medicine, Department XI (Pediatrics II), 2 Eftimie Murgu Sq., 300041, Timisoara, Romania

² “Victor Babes” University of Medicine and Pharmacy, Faculty of Medicine, Department V (Internal Medicine I), 12 Revolutiei din 1989 Blvd., 300041, Timisoara, Romania

³ “Victor Babes” University of Medicine and Pharmacy, Faculty of Pharmacy, Department I (Analytical Chemistry), 2 Eftimie Murgu Sq., 300041, Timisoara, Romania

Abstract: *The monoclonal antibody bevacizumab, which neutralizes vascular endothelial growth factor, significantly affects the migration, survival, and proliferation of cells - all of which are critical for the growth and spread of tumors. The current study's objective was to create polyurethane structures that are more soluble in water so they may be employed as this active agent's transmembrane carrier. A polymer drug delivery system was created using an aliphatic isocyanate and a combination of ether and ester polyols, resulting in a suitable release profile and membrane penetrability. The solubility, pH, and refractivity index measurements, the size distribution and surface charge, the encapsulation efficacy and release profile, the proliferation of cells, and skin irritation tests on mice were used to describe the two samples. Our findings reveal that nearly neutral acido-basic polymer structures were achieved, ranging in size from 187 to 423 nm. Zeta potential values suggest a minor alteration in the propensity to form clusters in the sample with increased solubility, and UV-Vis analyses demonstrate an approximately 63±2% encapsulation efficacy. In terms of the samples' biosafety profile, the tests conducted on mouse skin and cell cultures did not result in significant adverse effects at the concentrations that were examined. The results of this preclinical investigation indicate that adding polar groups to polyurethane macromolecular chains improves aqueous solubility without changing the polymer carrier's other properties.*

Keywords: *cells culture, drug delivery, mice skin, UV-Vis, Zetasizer*

1. Introduction

Bevacizumab, also known as Avastin (BVZ, Figure 1), is a humanized monoclonal antibody medication that serves as a first-line therapy for the treatment of lung cancer, ovarian cancer, colon cancer, and age-related macular degeneration, a particular eye disease. The US Food and Drug Administration (FDA) approved this medication twenty years ago; the drug functions as an angiogenesis inhibitor by repressing vascular endothelial growth factor A (VEGF-A) [1].

The need for alternative routes of administration for drugs utilized in cancer treatment is of utmost importance due to the ongoing challenges in effectively managing this disease. Despite advancements in cancer research, the disease remains a leading cause of mortality worldwide. One of the primary challenges faced by cancer therapy is the lack of specificity in current treatment options, which can result in harmful side effects and toxicity [2]. Furthermore, the inherent diversity of cancer and the emergence of drug resistance dictate the need for continuous exploration of innovative therapeutic options [3]. On the other side, BVZ has been associated with several effects, including nosebleeds, headaches, elevated blood pressure, rashes, gastrointestinal perforations, allergic reactions, blood clots, vision loss, and retinal detachment [4].

Drug delivery systems (DDSs) are integral to modern therapeutic strategies, enhancing the efficacy of treatments by ensuring that drugs are delivered to the targeted area within the body with precision, thereby maximizing therapeutic effects and minimizing off-target accumulation [5].

*[email:borcan.cristina@umft.ro](mailto:borcan.cristina@umft.ro)

These systems are particularly vital in chemotherapy, where targeted delivery to specific organs, tissues, or cells can significantly improve treatment outcomes by reducing the impact on healthy tissues [6]. Moreover, while traditional drug carriers have offered a more monotonic control over drug release, advancements in DDS now allow for "programmed" and "on-demand" drug release, providing a more sophisticated control over the timing, dosage, and location of drug administration [7]. Furthermore, sustained-release DDS have evolved to incorporate novel materials and technologies, enabling personalized medicine approaches that tailor drug delivery to individual patient needs [8].

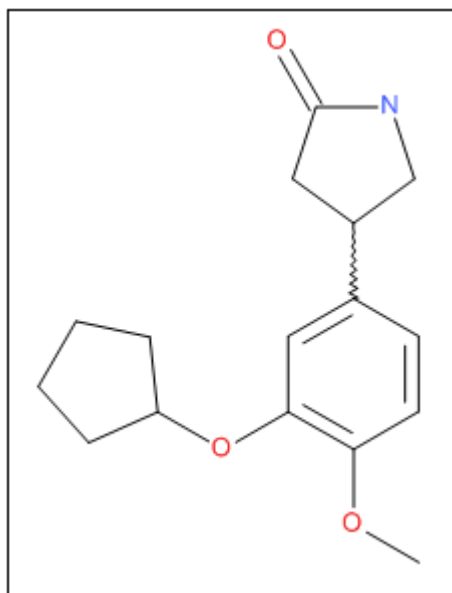


Figure 1. Chemical structure of BVZ

Polyurethanes (PUs) are a class of polymers that have garnered significant attention in the medical and pharmaceutical fields due to their versatility and range of applications. PU is widely used in biomaterial engineering, where their biodegradable and non-biodegradable variants serve as crucial components in DDS for cancer therapy [9]. The importance of PUs lies in their ability to synthesize specific building blocks, allowing for the creation of materials with tailored physicochemical and biological properties. This customization facilitates the development of anti-cancer DDSs with advantages such as high pharmacological efficiency, low toxicity, and tumor-targeting capabilities [9]. Interestingly, while PUs are highlighted for their role in oncological applications, they are part of a broader spectrum of polymeric materials used in drug delivery. These materials are rapidly emerging in pharmaceutical fields due to their biocompatibility and ability to act as carriers for potent anticancer drugs [10]. The use of biodegradable polymers, in particular, represents a new dimension in polymeric DDSs, with clinical applications that underscore their potential importance [11]. Unfortunately, the weak solubility of PUs in aqueous media can be described as a disadvantage in DDS due to the possible limitations it imposes on the bioavailability and administration of therapeutic agents. Solubility is a critical factor in the design of DDS, as it influences the drug's ability to be absorbed into the systemic circulation and reach the target site in the body. Poor solubility can lead to challenges in formulating effective delivery vehicles that maintain the stability and controlled release of the drug [12]. Interestingly, while the inherent low solubility of PUs in water is a drawback, it is also associated with certain advantages. For instance, the hydrophobic nature of PUs can be leveraged to create sustained-release formulations, where the slow diffusion of the drug from the polymeric matrix results in prolonged therapeutic effects [13]. Additionally, modifications to the PU structure, such as the incorporation of hydrophilic segments or the use of additives, can enhance solubility and modulate drug release profiles [14].

Our research team commenced investigating the encapsulation of BVZ within polyurethane carriers a decade ago [15, 16]. Concurrently, we extensively explored methods for increasing the aqueous



solubility of polyurethane carriers and patented an idea involving the incorporation of polar groups into macromolecular chains [17]. The current paper aimed to present the results of the synthesis and preliminary characterization of modified PU structures with potential applications as drug delivery systems for BVZ. The primary contribution of this research lies in the incorporation of polar functional groups into macromolecular chains and the subsequent assessment of their influence on the relevant characteristics of the resultant product. The originality of this formulation lies in the synthesis of a polyurethane carrier without the use of catalysts; in the PU industry, catalysts typically consist of organometallic compounds that contain hazardous heavy metals or extremely reactive tertiary amines, which can cause severe irritation or even burns.

2. Materials and methods

2.1. Raw materials

Sorbitan trioleate, also known as Span[®] 85, and 1,2-propanediol, 2-acetate were procured from Sigma (Taufkirchen, Germany). Other raw materials included isophorone diisocyanate (IPDI), polyethylene glycol (PEG 400), polycaprolactone diol (PCL Mn~530), 1,6-hexanediol (HD), tris-(hydroxymethyl)amino-methane (THAM), inorganic compounds (NaCl, KCl, MgCl₂, Na₂HPO₄, K₂HPO₄, KH₂PO₄, and NaHCO₃), and bevacizumab (BVZ) from Sigma Aldrich (St Louis, USA), and acetone from Honeywell Riedel-de Haen (Seelze, Germany). The chemicals were of analytical grade purity and were utilized without any prior purification, and a JP Selecta Dest-4 distiller was employed to obtain double-distilled water.

For the assessment of cytotoxicity, the HDFa (Human Dermal Fibroblast) cell line was procured from Invitrogen (Waltham, USA), while all the reagents (culture media, antibiotics, FBS, PBS, trypsin-EDTA, and MTT solution, DMSO) and culture supplies (flasks, Pasteur pipettes, pipette tips, microplates) were obtained from Thermo Fischer Scientific (Waltham, USA).

Male, 9-week-old CB17SCID mice were obtained from Charles River (Sulzfeld, Germany). They were maintained under standard conditions: temperature (24±2°C), humidity (55±5%), and a 12h light/dark cycle. The mice were provided with *ad libitum* access to food and water throughout the experiment.

2.2. Synthesis of the carrier

The synthesis of PU is based on a polyaddition reaction between an active hydrogen-containing phase, consisting of ether- and/or ester-polyols, and a di-isocyanate. In this study, an aliphatic isocyanate (IPDI) was utilized as the organic phase due to its non-carcinogenic potential. The aqueous phase was composed of a specific ratio between PEG 400 and PCL, determined by previous research findings [18, 19] and the understanding that this ratio has a significant impact on drug release kinetics.

The inorganic phase, comprising 1.8 mL of HD, 3.5 g of PEG 400, 3.0 g of PCL, 1.2 g of THAM, 1.5 mL of Span[®] 85, and 0.5 mg of BVZ, was dissolved in 35.0 mL of double-distilled water and stirred at 315 rpm and 30±0.2°C overnight. Concurrently, a solution based on 6.0 mL of IPDI in 25.0 mL of acetone was homogenized in a separate flask at 365 rpm and 30±0.2°C for 120 min. The inorganic phase was then poured quickly in this last flask, and the content was stirred at 300 rpm at room temperatures for 3 h to complete the synthesis of the macromolecular chains. A P700 Universal thermometer from Dostmann electronic GmbH (Wertheim, Germany) was employed to precisely check the temperatures. Finally, the content of the flask was sonicated for 5 min using a Bandelin Sonorex Digitec bath sonicator (Berlin, Germany).

To create two samples for a comparative characterization, the whole process was done twice: PU₀, which served as a reference sample, and PU₁, which was an enhanced sample that included 0.2 g of 1,2-propanediol, 2-acetate in the inorganic phase.

The concluding stage necessitated filtering the gathered suspensions through 0.22 μm PVDF sterile syringe filters from Merck Millipore (Darmstadt, Germany) while simultaneously employing a washing process comprised using a mixture of water and acetone (1:1.3, v/v). Following this, the suspensions

were centrifuged at 2,200 G using an Ika Mini G microcentrifuge (Staufen, Germany) to enhance the concentration of the samples. The water-acetone mixture utilized during the washing process was subsequently analyzed to determine the free BVZ content. Ultimately, the samples were dried in borosilicate glass Petri dishes at room temperature until they had reached a consistent mass (approximately 120 h).

2.3. The stability of samples

Each sample was stored at three different temperatures for a month ($8\pm 0.5^\circ\text{C}$, $25\pm 0.5^\circ\text{C}$, and $40\pm 0.5^\circ\text{C}$) with $65\pm 3\%$ relative humidity. An aliquot of each sample was used to measure its stability. Samples were recorded every week for color and electrical conductivity using a SI Analytics UVi Line 9400 spectrophotometer (Mainz, Germany) and a Jenway Bench 4010 Conductivity meter (Staffordshire, UK) at 25°C in aqueous solutions (0.8 mg mL^{-1}).

2.4. Physico-chemical characteristics

The pH of each sample was evaluated using a Mettler Toledo FiveGo F2 portable pH meter (Schwerzenbach, Switzerland), along with InLab[®] Expert Go Sensor and aqueous solutions containing the same concentration (0.8 mg mL^{-1}) at a temperature of 25°C .

To determine the refractive index of the synthesized samples, 2-3 drops of each aqueous solution were used with a Kern digital refractometer (Balingen, Germany) at room temperature.

The solubility of samples in water, acetone, and DMSO was assessed according to a procedure already described by our team [20]. Five milligrams of dried product were dissolved in 20 mL glass vials with screw caps in each respective solvent at room temperature. The volume of each solvent was recorded when a single, clear liquid phase was observed without any distinct solid or gel particles present.

2.5. Drug loading

The efficiency of the BVZ encapsulation was calculated by reporting the quantity of the free drug to the total added amount, (1):

$$\text{DL}\% = \frac{\text{TA} - \text{FD}}{\text{TA}} \cdot 100 \quad (1)$$

where DL% is the drug loading percentage, TA and FD are the total amount and the amount of free drug (mg).

These amounts were calculated using the absorption spectra of BVZ (Figure 2a) and the Beer-Lambert law: a calibration curve (the absorption values vs. drug concentration, Figure 2b) was initially drawn.

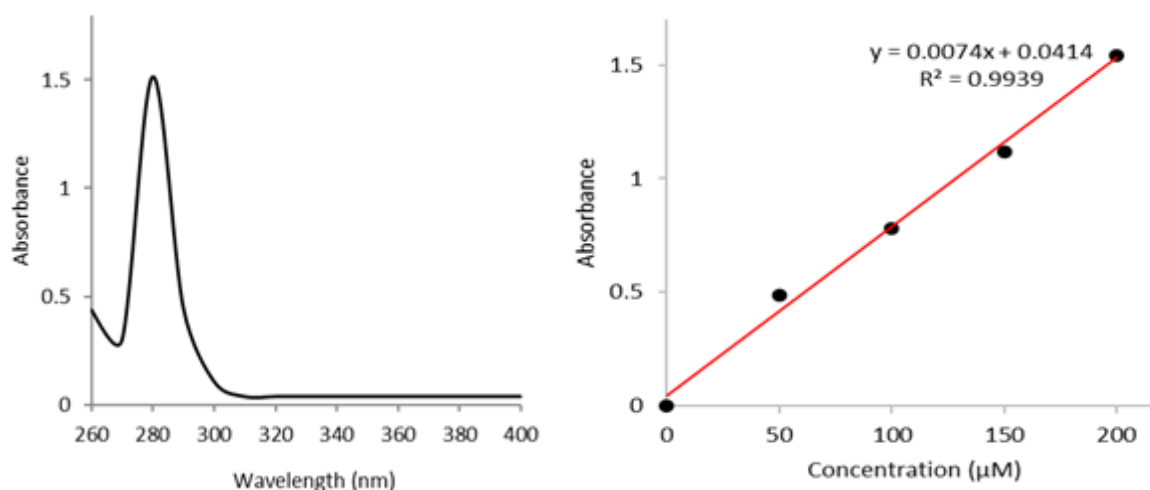


Figure 2. (a) UV spectra of pure BVZ and (b) calibration curve (linearity) of BVZ at 280 nm



2.6. Drug release profile

The amount of BVZ released during the exposure of samples to a simulated body fluid (SBF) was monitored to obtain the profile of cumulative drug release (CDR). The SBF was prepared according to the method described by F. Baino and S. Yamaguchi [21]. The SBF comprised of 6.6 g NaCl, 2.3 g NaHCO₃, 0.4 g KCl, 0.1 g Na₂HPO₄ mixed with 960 mL double distilled water in a 1000 mL-capacity flat bottom flask. The mixture was heated at 37 °C and 0.3 g MgCl₂ hexahydrate, 0.4 g CaCl₂ dihydrate, 0.1 g Na₂SO₄, 6.1 g Tris were added. The pH was then adjusted to 7.4 with 1M HCl. The samples were maintained in the SBF at 37.0±0.5°C and 150 rpm for 5 days. The CDR was determined using UV-Vis spectroscopy by replacing 1.0 mL of the SBF with fresh degrading environment daily. The analysis was carried out based on a calibration curve of absorption vs. concentration of BVZ in SBF ($y = 0.0068x + 0.0325$, $R^2 = 0.9916$).

2.7. The penetrability rate

A Franz-cell with a diffusion area of 1.77 cm², a receptor volume of 12.0 mL, and an inner diameter of 15 mm, was utilized to evaluate the carrier permeation. The receptor chamber was filled with PBS, and the experiment was carried out at a temperature of 25±1°C; every 10 h, 1.0 mL of liquid from the receptor chamber was replaced with fresh buffer, and spectral analysis was conducted.

2.8. Zetasizer tests

The size and surface charge of the PU structures were assessed using dynamic light scattering on a Cordouan Technol. system (Pessac, France). The main input parameters that were set for the determination of particles size and its distribution included the temperature (25°C), time interval (16-18 μs), channels number (440-460), laser power (70-80 %), acquisition mode (continuous), and analysis mode (Pade-Laplace). The following parameters were set to detect surface charge: temperature (25°C), applied field (automatic), medium resolution (0.8 Hz), number/sequence (5), laser power (70-80 %), Henry function (Smoluchowski), and cuvettes (quartz).

2.9. Cells viability

The viability of HDFa cells was determined using the MTT assay. The cells were seeded in culture medium supplemented with 10% FBS and 1% penicillin-streptomycin, and the medium was changed after 2-3 days. The cells (1.5·10⁵ cells/mL) were seeded in 100 μL of medium in 96-well plates and allowed to adhere for 24 h in an incubator. After 24 h, the growth medium was replaced with the obtained samples (90 μL medium+10 μL sample), and the tests were conducted in triplicate at 24 and 72 h after the treatment.

2.10. Skin irritation evaluations

12 mice were split up into four groups, for the two samples respectively two special groups (“SLS”, which received treatment with 2.0% sodium lauryl sulfate solution, a known skin irritant, and “control”, which received simply the solvent treatment). At the start of the experiment and thereafter every five days, the back hair of the CB17SCID mice (about 3 cm²) was shaved. The parameters were measured half an hour after the application of the tested compounds (40±5 μL once) every third day for 15 days. Using a Multiprobe Adapter System (MPA5) from Courage+Khazaka electronic GmbH (Cologne, Germany) fitted with Mexameter[®] MX 18 and Corneometer[®] CM 825 probes, changes in skin erythema and moisture were tracked. The research was done according to all ethical principles for studies on animals; the procedure was evaluated and approved by the Ethical Committee of “Victor Babes” University of Medicine and Pharmacy Timisoara, Romania.

2.11. Statistics

Data analyses were performed using IBM SPSS Software version 27.0.0.0 (Armonk, NY, USA). Continuous variables are presented as mean and standard error (SE). Non-parametric tests were used to

evaluate the significance of the small datasets. Statistical significance was set at $P < 0.05$. The charts were modeled using OriginPro 2018 (Northampton, MA, USA).

3. Results and discussions

3.1. Stability of PU carrier

Although it is commonly recognized that polymer materials show remarkable durability over time, certain degradation processes caused by heat, UV light, microbial assault, and hydrolytic conditions can change the characteristics of macromolecule-based biomaterials [22]. One important factor that indicates regulated storage circumstances, such as humidity, temperature, exposure to sunlight, etc., is the stability of a pharmaceutical formulation. Table 1 displays the color and electrical conductivity variations of the samples.

Table 1. The changes of maximum absorbance and electrical conductivity levels in 30 days

Sample	Percentual changes at different temperature, %					
	8±0.5 °C		25±0.5 °C		40±0.5 °C	
	abs.	cond.	abs.	cond.	abs.	cond.
PU_0	4.5	7.6	4.1	7.2	4.1	6.9
PU_1	4.4	8.0	3.9	7.7	4.0	7.8

The position of maximum absorption in UV-Vis spectra is influenced by several factors, including the nature of the chromophore, the presence of auxochromes, the degree of conjugation and unsaturation, steric hindrance, the concentration of the solute, and environmental conditions such as pH and temperature [23]. These factors can cause shifts and changes in the absorption spectra, which are important for the qualitative and quantitative analysis of chemicals. Changes between 4.0-4.5% were observed in the case of our samples for the maximum absorbance peaks and between 6.9 and 8.0% for the electrical conductivity. Based on this analysis, the carrier is more stable at 25 and 40°C; it can be inferred that these products are suitable for storage at room temperature.

3.2. pH measurements

The pH values of samples were determined in triplicate; the obtained values are presented in Table 2 for each sample.

Table 2. The pH values recorded for each sample

Sample	Evaluation		
	1	2	3
PU_0	6.63	6.81	6.70
PU_1	6.61	6.34	6.41

The following average values were found: 6.71 for PU_0 and 6.45 for sample PU_1 and they indicate that the tested samples exhibit weak acidic properties. The data indicates that these structures are suitable for delivery through multiple routes of administration.

3.3. Refractivity index

Analogous to pH monitoring, the refractive index was measured three times for each sample. Table 3 displays the obtained values.

Table 3. The refractivity index found for each sample

Sample	Evaluation		
	1	2	3
PU_0	1.60	1.60	1.59
PU_1	1.58	1.59	1.58

Therefore, average refractivity index values of 1.60 for sample PU_0 and 1.58 for sample PU_1 were obtained. Wang et al. [24] reported the synthesis of PU structures with a refractive index of 1.64, which can be utilized as light-trapping material with broad anti-reflection performance. A review published several years ago also presented refractive index values between 1.4 and 1.6 for PU structures [25].

3.4. Sample solubility

Multiple solubility measurements of samples in various solvents were conducted to determine the effect of polar groups incorporated into the macromolecular chains. Table 4 displays the solubility of synthesized samples in different solvents.

Table 4. Comparative solubility of samples

Sample	Solubility (mg mL ⁻¹)		
	water	acetone	DMSO
PU_0	0.81	1.06	1.08
PU_1	2.07	0.95	0.89

Despite the significant advantages of polymeric drug delivery systems, their limited aqueous solubility remains a primary limitation, as previously discussed in our prior publications [15-20]. In the current study, the incorporation of polar functional groups onto the macromolecular structure of carrier molecules results in improved solubility within aqueous environments.

3.5. Drug loading

The percentage of BVZ that was encapsulated within the PU structures is known as the encapsulation efficiency. The two main parameters in this field are the controlled release behavior and the encapsulation efficiency, and they are primarily dependent on the forces between molecules and the chemical structure. The average encapsulation efficiencies in the present investigation are 61.9% (PU_0) and 65.1% (PU_1).

3.6. Drug release profile

The cumulated drug release is presented in Figure 3.

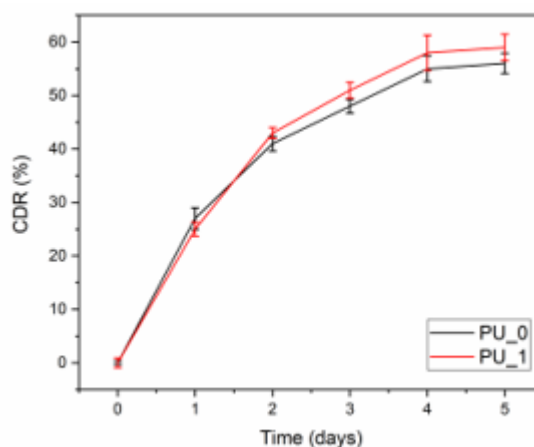


Figure 3. Comparative cumulated drug release

One tool for comprehending the kinetics and mechanism of release is the drug release profile. Numerous parameters, including the drug and carrier's physico-chemical characteristics, their interaction, the DDS's shape, and environmental variables like pH and temperature, all affect the release. Our curve's form shows that there is a burst release on the first day, a regulated or steady release throughout the next three days, and a lag phase at the end. The similarity between the two samples is

demonstrated by the current graph, so the addition of polar functional groups has no effect on this parameter.

3.7. Penetrability rate

A complex mixture of proteins and various lipid species, including glycerophospholipids, sphingolipids, and cholesterol, make up body membranes. The permeation of active compounds through membranes is an important factor that affects their release profile and bioavailability. Our findings indicate that both samples exhibited satisfactory permeation through artificial membranes (Figure 4). However, the most promising results were obtained with sample PU_0, which demonstrated more than 75% permeation within the first two days.

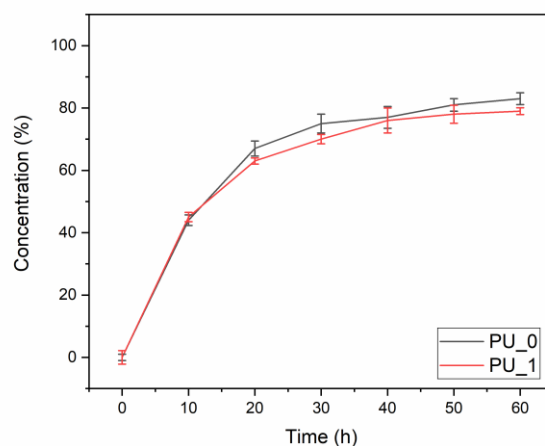


Figure 4. Comparative penetrability rates

Active agents and drugs that are small enough can passively diffuse across membranes. Polar transmembrane carriers are used to facilitate the transport of bigger molecules [26]. The gradually increasing slope indicates a rise in permeation at the beginning of the curve. The structures that seeped into the Franz-cell are the cause of this phenomena. More molecules gradually permeate into the receptor chamber as the permeation from the first chamber deepens. As a result, as the center section of the curve shows, the permeation keeps growing. The permeation reached a critical point after 30-40 h, almost reaching a plateau; this phenomenon is explained by the concentrations of the structures reaching equilibrium.

3.8. Zetasizer

Dynamic light scattering analysis is often used to analyze colloidal suspensions and solutions; surface charge, dispersity (PDI), and particle size are crucial factors in drug administration and bioavailability. Table 5 shows the values obtained in the Zetasizer assessment.

Table 5. Comparative Zetasizer characterization

Sample	Analyzed parameters		
	size (nm)	PDI	Zeta potential (mV)
PU_0	206±19 (100%)	0.36	+26.1
PU_1	187±11 (37%) 423±15 (63%)	0.78	+27.9

Table 5 illustrates that sample PU_1 consist of a disperse system comprising two distinct particle populations, whereas sample PU_0 exhibits a more homogeneous system based on a single population of particles. The benefits of using a polydisperse system as a drug carrier have been explained in the

literature by Błaszczuk et al. [27]; their study showed that carriers of different sizes can promote prolonged release, while monodisperse systems are expensive and difficult to produce on an industrial scale. According to Clogston and Patri, systems with a mild disposition to produce agglomerations are linked to Zeta potentials between +10 and +30 mV, whereas structures with a high impulse are unique to the values between -10 and +10 mV [28]. Thus, the current average values of Zeta potential are also indicative of systems with a medium resistance to the tendency to form particle clusters in both samples.

3.9. Cells viability

Figure 5 shows the HDFa cells proliferation rate.

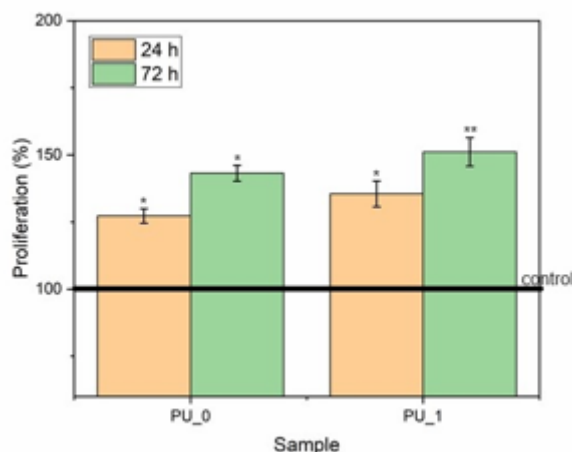


Figure 5. Comparative cells proliferation; one-way ANOVA was executed (* $p < 0.05$ and ** $p < 0.01$ vs. control)

At 24 and 72 h, the rates of cell growth were examined (Figure 5). Both samples showed higher cell proliferation after 24 h (around 135% compared to the control, which was established at 100%). Both samples showed the same pattern of enhanced cell growth after 72 h of incubation. According to previous research conducted by our team [29], the proliferative effects of polyurethane structures have been previously documented in the scientific literature. In summary, our findings suggest that the synthesized samples do not display any cytotoxic effects.

3.10. Skin irritation evaluation

Figures 6 and 7 present the evolutions of erythema and skin hydration during a 15-day evaluation.

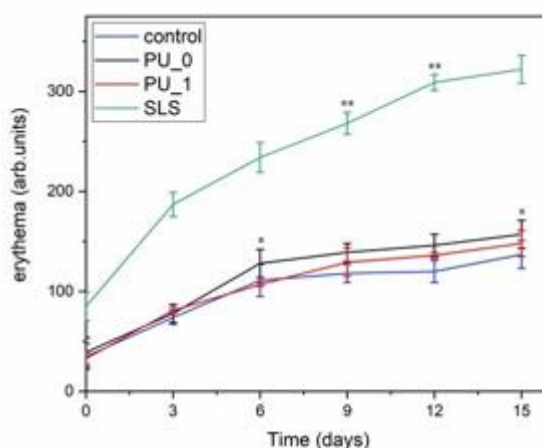


Figure 6. Changes in erythema levels; one-way ANOVA test was performed, followed by Dunnet's test (* $p < 0.05$ and ** $p < 0.01$ vs. control)

Mice skin models are frequently used to assess if new samples have the potential to induce skin irritation, which manifests as swelling, redness, skin dehydration, inflammation, and sometimes discomfort or itching. In these models, test compounds are applied topically to the mice's skin, and the irritation is then measured using a variety of non-invasive testing techniques. It should be noted that individual mice have varying levels of sensitivity to irritation. Furthermore, the magnitude of the alterations in skin characteristics is quite significant. The synthesized samples are safe for use on people, according to our findings, which are consistent with those reported in the literature [30].

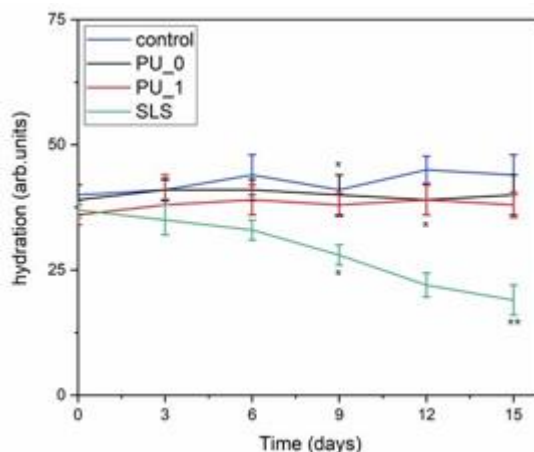


Figure 7. Comparative changes of skin hydration; one-way ANOVA test was performed, followed by Dunnet's test (* $p < 0.05$ and ** $p < 0.01$ vs. control)

4. Conclusions

To effectively manage and cure diseases, drug delivery systems play an important role in increasing therapeutic efficacy, decreasing toxicity, and increasing patient compliance. In addition to improving medication delivery, polymer carriers are crucial for meeting the specific demands of each patient, considering things like circadian cycles and pharmacogenomics.

This study details the creation of a novel polyurethane carrier that facilitates BVZ transmembrane transport. Two samples that are based on a combination of polyethylene glycol and polycaprolactone diol and a non-carcinogenic diisocyanate have been produced and subjected to comparative analysis. The modified sample, containing polar functional groups in its macromolecular chains, has weakly acidic characteristics ($pH = 6.45 \pm 0.14$) and is a disperse system ($PDI = 0.78$) with mean particle sizes ranging from 187 to 423 nm. Furthermore, there is no significant difference in the pH , refractive index, encapsulation efficiency, or penetration rate when polar groups are added. The data from the cytotoxicity and irritation potential evaluations suggest that the obtained samples are not harmful to humans: the viability of adult fibroblasts has risen, while there were no appreciable changes in skin erythema or moisture when compared to the reference values.

Our findings showed how polyurethane-based drug delivery systems with increased aqueous solubility can be used for monoclonal antibodies.

Future directions for this study will focus on creating more sophisticated polyurethane-based drug delivery systems that can efficiently provide a variety of therapeutic agents, such as peptides, small molecules, and other biologics, for a range of illnesses and ailments. To assess the long-term safety and effectiveness of these systems in preclinical and clinical settings, more research is also required.

Acknowledgments: The authors would like to acknowledge “Victor Babes” University of Medicine and Pharmacy Timisoara for their support in covering the costs of publication for this research paper.



References

1. TAIRA, K., OKAZAKI, S., AKIYOSHI, K., MACHIDA, H., IKEYA, T., KIMURA, A., NAKATA, A., NADATANI, Y., OHMINAMI, M., FUKUNAGA, S., OTANI, K., HOSOMI, S., TANAKA, F., KAMATA, N., NAGAMI, Y., FUJIWARA, Y., Short bevacizumab infusion as an effective and safe treatment for colorectal cancer, *Mol. Clin. Oncol.*, **17**(3), 2022, 139. <https://doi.org/10.3892/mco.2022.2572>.
2. BOJÓRQUEZ, N.D.C.Q., CAMPOS, M.R.S., Traditional and Novel Computer-Aided Drug Design (CADD) Approaches in the Anticancer Drug Discovery Process, *Curr. Cancer Drug Targets*, **23**(5), 2023, 333-345. <https://doi.org/10.2174/1568009622666220705104249>.
3. SONG, Q., ZHANG, W., SHI, D., ZHANG, Z., ZHAO, Q., WANG, M., HUANG, M., MENG, J., CUI, W., LUO, X., Overexpression of cannabinoid receptor 2 is associated with human breast cancer proliferation, apoptosis, chemosensitivity and prognosis via the PI3K/Akt/mTOR signaling pathway, *Cancer Med.*, **12**(12), 2023, 13538-13550. <https://doi.org/10.1002/cam4.6037>.
4. WANG, L., FEI, Y., QU, H., ZHANG, H., WANG, Y., WU, Z., FAN, G., Five years of safety profile of bevacizumab: an analysis of real-world pharmacovigilance and randomized clinical trials, *J. Pharm. Health Care Sci.*, **10**(1), 2024, 1. <https://doi.org/10.1186/s40780-023-00314-w>.
5. HOQUE, M., SAHA, S.N., AKRAM, T., Nanogels Based Drug Delivery System: A Promising Therapeutic Strategy, *Int. J. Pharm. Sci.*, **1**(11), 2023, 103-111. <https://doi.org/10.5281/zenodo.10070861>.
6. SETIA, A., VALLAMKONDA, B., CHALLA, R.R., MEHATA, A.K., BADGUJAR, P., MUTHU, M.S., Herbal Theranostics: Controlled, Targeted Delivery and Imaging of Herbal Molecules, *Nanotheranostics*, **8**(3), 2024, 344-379. <https://doi.org/10.7150/ntno.94987>.
7. DAVOODI, P., LEE, L.Y., XU, Q., SUNIL, V., SUN, Y., SOH, S., WANG, C.-H., Drug delivery systems for programmed and on-demand release, *Adv. Drug Deliv. Rev.*, **132**, 2018, 104-138. <https://doi.org/10.1016/j.addr.2018.07.002>.
8. EZIKE, T.C., OKPALA, U.S., ONOJA, U.L., NWIKE, C.P., EZEAKO, E.C., OKPARA, O.J., OKOROAFOR, C.C., EZE, S.C., KALU, O.L., ODOH, E.C., NWADIKE, U.G., OGBODO, J.O., UMEH, B.U., OSSAI, E.C., NWANGUMA, B.C., Advances in drug delivery systems, challenges and future directions, *Heliyon*, **9**(6), 2023, e17488. <https://doi.org/10.1016/j.heliyon.2023.e17488>.
9. SOBCZAK, M., KĘDRA, K., Biomedical Polyurethanes for Anti-Cancer Drug Delivery Systems: A Brief, Comprehensive Review. *Int. J. Mol. Sci.*, **23**(15), 2022, 8181. <https://doi.org/10.3390/ijms23158181>.
10. SUNG, Y.K., Kim, S.W., Recent advances in polymeric drug delivery systems, *Biomater. Res.*, **24**, 2020, 12. <https://doi.org/10.1186/s40824-020-00190-7>.
11. TSUNG, T.-H., TSAI, Y.-C., LEE, H.-P., CHEN, Y.-H., LU, D.-W., Biodegradable Polymer-Based Drug-Delivery Systems for Ocular Diseases, *Int. J. Mol. Sci.*, **24**, 2023, 12976. <https://doi.org/10.3390/ijms241612976>.
12. HARSHITA, BARKAT, M.A., DAS, S.S., POTTOO, F.H., BEG, S., RAHMAN, Z., Lipid-Based Nanosystem As Intelligent Carriers for Versatile Drug Delivery Applications, *Curr. Pharm. Des.*, **26**(11), 2020, 1167-1180. <https://doi.org/10.2174/1381612826666200206094529>.
13. LOWINGER, M.B., BARRETT, S.E., ZHANG, F., WILLIAMS, R.O.III, Sustained Release Drug Delivery Applications of Polyurethanes, *Pharmaceutics*, **10**, 2018, 55. <https://doi.org/10.3390/pharmaceutics10020055>.
14. SONG, W., MUHAMMAD, S., DANG, S., OU, X., FANG, X., ZHANG, Y., HUANG, L., GUO, B., DU, X., The state-of-art polyurethane nanoparticles for drug delivery applications, *Front. Chem.*, **12**, 2024, 1378324. <https://doi.org/10.3389/fchem.2024.1378324>.
15. ALBULESCU, R.C., BORCAN, F., PUIU, M., Development of polymeric carriers used for bevacizumab - a possible remedy in retinopathy of prematurity, *Int. J. Adv. Pharm.*, **4**(3), 2014, 154-159.



16. ALBULESCU, R.C., BORCAN, F., PAUL, C., VELEA, I., PUIU, M., Development and in vitro evaluation of polyurethane microparticles as carrier for bevacizumab: an alternative treatment for retinopathy of prematurity, *Int. Curr. Pharm. J.*, **3**(6), 2014, 275-279.
17. *** UMF TIMISOARA (BORCAN, F., DEHELEAN, C.A., SOICA, C.M.), [Procedeu de obținere a unui transportor transdermic al aciclovirului], Patent RO134816 / 30.06.2023.
18. CITU, C., CEUTA, L., POPOVICI, R., IONESCU, D., PINZARU, I., BORCAN, F., Alternative Possibilities to Assess a Phytohormone Release Rate from a Polyurethane Carrier. *Mater. Plast.*, **52**(4), 2015, 553-559.
19. MOLERIU, L., DUSE, A.O., BORCAN, F., SOICA, C., KURUNCZI, L., NICOLOV, M., MIOC, M., Formulation and characterization of anti-bacterial hydrogels based on polyurethane microstructures and 1,2,4-triazole derivatives, *Mater. Plast.*, **54**(2), 2017, 348-352.
20. BORCAN, F., CHIRITA-EMANDI, A., ANDREESCU, N.I., BORCAN, L.C., ALBULESCU, R.C., PUIU, M., TOMESCU, M.C., Synthesis and preliminary characterization of polyurethane nanoparticles with ginger extract as a possible cardiovascular protector, *Int. J. Nanomedicine.*, **14**, 2019, 3691-3703. <https://doi.org/10.2147/IJN.S202049>.
21. BAINO, F., YAMAGUCHI, S., The Use of Simulated Body Fluid (SBF) for Assessing Materials Bioactivity in the Context of Tissue Engineering: Review and Challenges, *Biomimetics (Basel)*, **5**(4), 2020, 57. <https://doi.org/10.3390/biomimetics5040057>.
22. SILVA, R.R.A., MARQUES, C.S., ARRUDA, T.R., TEIXEIRA, S.C., DE OLIVEIRA, T.V., Biodegradation of Polymers: Stages, Measurement, Standards and Prospects, *Macromol.*, **3**, 2023, 371-399. <https://doi.org/10.3390/macromol3020023>.
23. PRABHUMIRASHI, L.S., KUNTE, S.S., Solvent effects on electronic absorption spectra of nitrochlorobenzenes, nitrophenols and nitroanilines II. Studies in polar solvents, *Spectrochim. Acta A Mol. Spectrosc.*, **44**(2), 1988, 213-220. [https://doi.org/10.1016/0584-8539\(88\)80245-9](https://doi.org/10.1016/0584-8539(88)80245-9).
24. WANG, S., CUI, H., JIN, S., PI, X., HE, H., SHOU, C., YANG, D., WANG, L., Anti-reflection effect of high refractive index polyurethane with different light trapping structures on solar cells, *Heliyon.* **9**(9), 2023, e20264. <https://doi.org/10.1016/j.heliyon.2023.e20264>.
25. CHANDRINOS, A, A Review of Polymers and Plastic High Index Optical Materials, *J. Mat. Sci. Res. Rev.*, **4**(2), 2021, 185-198.
26. YANG, N.J., HINNER, M.J., Getting across the cell membrane: an overview for small molecules, peptides, and proteins, *Methods Mol. Biol.*, **1266**, 2015, 29-53. https://doi.org/10.1007/978-1-4939-2272-7_3.
27. BŁASZCZYK, M., SEK, J., PRZYBYSZ, Ł., Analysis of droplet displacement during transport of polydisperse emulsion as drug carriers in microchannels, *Microfluid. Nanofluid.*, **26**, 2022, 19. <https://doi.org/10.1007/s10404-022-02526-2>.
28. CLOGSTON, J.D., PATRI, A.K., Zeta potential measurement, *Methods Mol. Biol.*, **697**, 2011, 63-70. https://doi.org/10.1007/978-1-60327-198-1_6.
29. OPREAN, C., ZAMBORI, C., BORCAN, F., SOICA, C., ZUPKO, I., MINORICS, R., BOJIN, F., AMBRUS, R., MUNTEAN, D., DANCIU, C., PINZARU, I.A., DEHELEAN, C., PAUNESCU, V., TANASIE, G., Anti-proliferative and antibacterial in vitro evaluation of the polyurethane nanostructures incorporating pentacyclic triterpenes. *Pharm. Biol.*, **54**(11), 2016, 2714-2722. <https://doi.org/10.1080/13880209.2016.1180538>.
30. GURITA (CIOBOTARU), V.G., PAVEL, I.Z., BORCAN, F., MOACA, A., DANCIU, C., DIACONEASA, Z., IMBREA, I., VLAD, D., DUMITRASCU, V., POP, G., Toxicological Evaluation of Some Essential Oils Obtained from Selected Romania Lamiaceae Species in Complex with Hydroxypropyl – gammacyclodextrin, *Rev. Chim.*, **70**(10), 2019, 3703-3707.

Manuscript received: 04.07.2024